Reactive and Functional Polymers 169 (2021) 105088

Contents lists available at ScienceDirect

Reactive and Functional Polymers

journal homepage: www.elsevier.com/locate/react

Perspective Article

Semi-conducting cyclic copolymers of acetylene and propyne

Zhihui Miao [a,b], Alec M. Esper [a,b], Soufiane S. Nadif [b], Stella A. Gonsales [b], Brent S. Sumerlin [b,*], Adam S. Veige [a,b,*]

[a] Center for Catalysis, Department of Chemistry, University of Florida, P.O. Box 117200, Gainesville, FL 32611, United States
[b] George & Josephine Butler Polymer Research Laboratory, Center for Macromolecular Science & Engineering, Department of Chemistry, University of Florida, P.O. Box 117200, Gainesville, FL 32611, United States

ARTICLE INFO

Keywords:
Cyclic polymer
Copolymer
Polyacetylene
Polypropyne
Conductive polymers
Semi-conducting
Doping

ABSTRACT

Polyacetylene (PA) exhibits conductivities comparable to metals after doping, yet the extremely low solubility of PA limits its processing and utility. Introducing pendent groups can alter the properties of PA. Copolymerizing acetylene and propyne using Zieglar-Natta type catalysts affords linear poly(acetylene-*co*-propyne) as free-standing films. However, this process requires grams of catalysts and extensive workup. Cyclic polyacetylene is a unique topological isomer of linear polyacetylene. Herein, we report a facile synthesis of cyclic poly(acetylene-*co*-propyne) as thin, flexible films with extremely low catalyst loading (milligrams) and easy purification. Altering the feed ratio of acetylene and propyne produces copolymers with different acetylene/propyne incorporations. The films exhibit similar conductivities as linear copolymers after doping. The soluble portions of different cyclic copolymers exhibit low acetylene incorporation. TGA analysis reveals the cyclic copolymers are less thermally stable than cyclic PA, with the stability dependent on the ratio of acetylene and propyne incorporation.

1. Introduction

Polyacetylene (PA) is a conjugated polymer of great interest due to its metal-like conductivity upon doping. In 1958, Natta synthesized linear PA directly from acetylene producing an insoluble black bulk solid [1]. The insolubility and lack of thermal transitions made PA essentially uncharacterizable at that time. Later, Shirakawa demonstrated that coating a glass reactor with a thin layer of concentrated catalyst solution, followed by introducing acetylene gas, generated PA as a thin, flexible, and lustrous film that was semi-conducting [2,3]. Heeger, MacDiarmid, and Shirakawa also discovered that doping these PA films with halogen vapors increased their conductivities by orders of magnitude [4], transforming them from semi-conductors to conductors, in some cases, comparable to metal conductors after chain alignment [5,6]. While highly conductive, the notorious insolubility of PA and its lack of thermal transitions still limit its characterization, processibility, and thus, industrial utility [7]. Innovative indirect synthesis of PA provides better materials for characterization and processibility [8–14], yet the conductivity of polymers from indirect methods is lower than that of PA synthesized directly from acetylene monomer.

Other efforts to improve the solubility of PA include polymerizing substituted acetylenes, rendering the resulting polymers reasonably soluble [15]. Unfortunately, the bulkiness of these side groups forces the main chain to rotate, breaking the planarity of the backbone, and disrupting the conjugation [16]. Substituted polyacetylene homopolymers, therefore, forfeit the interesting physical properties stemming from highly conjugated π bonds, most importantly, conductivity. Alternatively, copolymers of acetylene and substituted alkynes are soluble and retain a highly conjugated backbone. Polymerizing monosubstituted cyclooctene via ring-opening metathesis polymerization (ROMP), Grubbs generated a substituted PA with a side group on every eighth carbon, which exhibited good solubility and a high conjugation length [17]. Adopting Shirakawa's method and introducing mixed acetylene and propyne feeds to Zieglar-Natta type catalysts, Chien et al. produced linear copolymers of acetylene and propyne as free-standing films [18]. Altering the gas feed ratios yielded copolymers with different acetylene and propyne content. Doping the copolymers with I_2 produces films with conductivities in the 10^{-2} to 10 Ω^{-1} cm^{-1} range, with decreasing conductivity as propyne content increases. Incorporating more propyne led to chain rotation, or "defects," in the π system, decreasing the conjugation length, increasing the bandgap, and ultimately reducing the electron carrier mobility of the backbone [18]. Supporting the

* Corresponding authors at: Department of Chemistry, University of Florida, P.O. Box 117200, Gainesville, FL 32611, United States.
E-mail addresses: sumerlin@chem.ufl.edu (B.S. Sumerlin), veige@chem.ufl.edu (A.S. Veige).

https://doi.org/10.1016/j.reactfunctpolym.2021.105088
Received 20 August 2021; Received in revised form 20 October 2021; Accepted 23 October 2021
Available online 29 October 2021

relationship between propyne incorporation and conductivity, EPR line widths correlated with a propyne-dependent decrease in conductivity.

The $Ti(O^nBu)_4/AlEt_3$ catalyst system used by Chien and coworkers requires a grams scale amount of $AlEt_3$ and $Ti(O^nBu)_4$, thus necessitating extensive washing (10–20 × 30 mL toluene) for catalyst removal after polymerization [18]. This laborious purification step arguably defeats the purpose of optimizing the processibility of these materials. In contrast, a tethered alkylidene catalyst developed in our labs, produces cyclic polyacetylene [19] and substituted polyacetylenes efficiently [20–26] (Scheme 1), with activities as high as 10^8 $g/mol_{cat}/h$ [27]. In addition to the potential interesting properties endowed from the cyclic topology [28–30], the cyclic PA synthesis employs low catalyst loadings of **1**. After synthesis the material only contains low amounts of residual metals requiring only three washes with THF [19]. Catalyst **1** also enables the synthesis of temporarily soluble cyclic PA, though ultimately the polymer produced suffers from the same insolubility of its famous linear derivative. While cyclic conducting macrocycles exist, these require palladium cross-couplings to make merely oligomers [31]. In this work. we report the first easily and catalytically synthesized soluble semi-conducting cyclic copolymers.

2. Experimental

2.1. Materials

Unless specified otherwise, all manipulations were performed under an inert atmosphere using glovebox or Schlenk line techniques. Tetrahydrofuran (THF) and toluene were dried using a GlassContour drying column. C6D6 (Cambridge Isotopes) and CDCl3 were dried over sodium-benzophenone ketyl, distilled or vacuum transferred, and stored over 3 Å molecular sieves. Acetylene was purchased from Airgas, passed through a cold trap of acetone and dry ice, a column of activated carbon, and 3 Å sieves prior to use. Propyne was purchased from Sigma-Aldrich. Complex **1** was prepared according to literature procedures [20]. Cyclic polyacetylene films were synthesized according to reported literature [19].

2.2. Synthetic procedures for copolymers

In a nitrogen-filled glove box, the bottom of a 20 mL vial was coated with a thin layer of solution comprising 2.0 mg of catalyst **1** dissolved in 400.0 μL of toluene. The vial was then sealed with a rubber septum. The septum was then pierced through with a plastic micropipette tip, and a flow adapter was place onto the septum. The connecting points were sealed with Teflon™ tape. The vial was then brought out of the glovebox with the flow adapter closed and placed in a fume hood. The flow adaptor was attached to a Schlenk line via rubber hosing, and the system was evacuated and flushed with argon three times. Under vacuum, quickly opening the flow adapter for three seconds then closing it placed

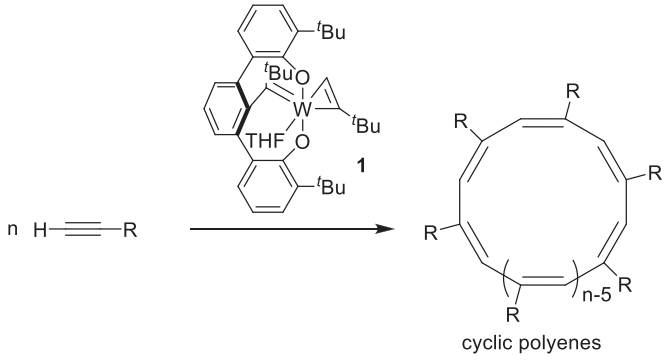

Scheme 1. Cyclic polyenes synthesis via ring expansion polymerization with catalyst **1**.

the vial under partial static vacuum. Acetylene and propyne cylinders were connected to the Schlenk line and the system was evacuated and flushed with argon three times. The system was evacuated up to the flow adaptor. The gases were admitted to the Schlenk line as needed to mix in the appropriate ratios using a Hg manometer. Opening the valve connected to the hose admitted the gas mixture up to the flow adaptor, the Hg level increased a few centimeters due to the static vacuum from the hose. Slowly opening the flow adapter introduced the mixed gas to the thin layer of catalyst solution. A black film formed immediately at the bottom of the vial, and the Hg level increased a few more centimeters due to the static vacuum from the vial and the gas consumption. After 15 min, the entire system was flushed with argon to remove the unreacted acetylene and propyne. The vial was then evacuated for 1 min and the flow adapter was closed to place the vial under static vacuum. The vial was then brought into the glovebox. Carefully lifting the film from the bottom of the vial followed by three washes with THF yields the cyclic copolymers synthesized with the desired comonomer mixture.

2.3. Doping of the cyclic copolymers

The copolymer films were exposed to I_2 in an evacuated iodine chamber for 3 h. The excess I_2 was removed by placing the films under dynamic vacuum overnight. The iodine doping weight percentages were calculated based on the weights before and after doping.

2.4. Conductivity measurement

The sheet resistivities of the films were measured on a Signatone Pro4-4400 4-point probe station equipped with a Keithley 2400 source meter. The thickness was measured using a profilometer. Measuring the sheet resistivity using a 4-point probe station and measuring the thickness with a profilometer gave the resistivity of the polyacetylene films. The conductivity was calculated as 1/resistivity.

2.5. NMR spectroscopy of the copolymers

A fraction of the copolymers were soluble and could be extracted by soaking the copolymers with 3 mL of THF over 24 h (10 wt% of $c\text{-}A_{75}\text{-}P_{25}$ and 28 wt% $c\text{-}A_{50}\text{-}P_{50}$). ^1H and ^{13}C NMR spectra were obtained on a Varian INOVA spectrometer (500 MHz). Chemical shifts, reported in δ (ppm), were referenced on the solvent, on the TMS scale for ^1H and ^{13}C.

The soluble portion of $c\text{-}A_{75}P_{25}$ gives a black solution in C_6D_6. ^1H NMR (Fig. 1, C_6D_6, 500 MHz) δ (ppm): 6.8–5.3 (b, 1.20H, =C-*H*), 2.1–0.9 (b, 3H, -C*H*$_3$). The soluble portion of $c\text{-}A_{50}P_{50}$ gives a deep red solution in C_6D_6. ^1H NMR (Fig. 2, C_6D_6, 500 MHz) δ (ppm): 6.9–4.9 (b, 1.22H, =C-*H*), 2.2–0.9 (b, 3H, -C*H*$_3$).

2.6. IR spectra of the cyclic copolymers

FT-IR was carried out using a Cary 630 FTIR spectrophotometer (Agilent Technologies, Santa Clara, CA, USA) in a glovebox. (See Fig. 3)

2.7. Resonance Raman Spectroscopy of the cyclic copolymers

The Raman spectra were recorded on a Horiba Aramis Raman system with a 10× object lens. Lasers with wavelengths of 633 nm and 785 nm and 600 g/mm and 1800 g/mm were used with a filter number of 0.6, a hole size of 200 μm, 1800 g/mm grating type, 1 s continuous mode time, and 1 s snapshot time. Fig. 7 depicts the Raman spectra of the copolymers.

2.8. TGA of the cyclic copolymers

Thermogravimetric analyses (TGA) were measured under nitrogen with a TGA Q5000 (TA Instruments). 5 mg portions of samples were heated at 20 °C/min from 25 to 600 °C. Fig. 8 depicts the TGA curves of

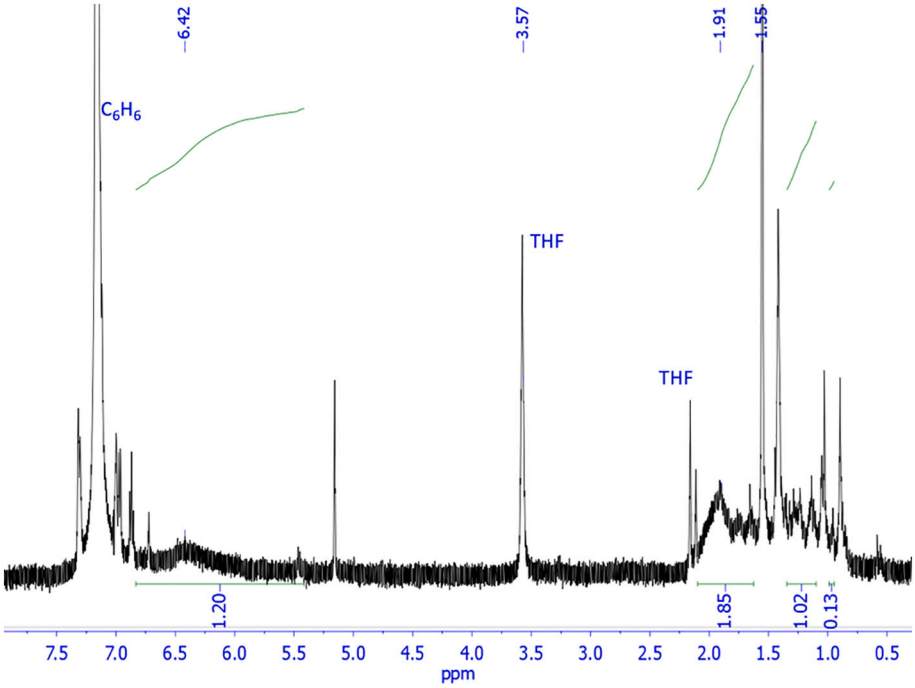

Fig. 1. ^{1}H NMR spectrum of the soluble portion of *c*-A_{75}-P_{25} in C_6D_6 at 25 °C.

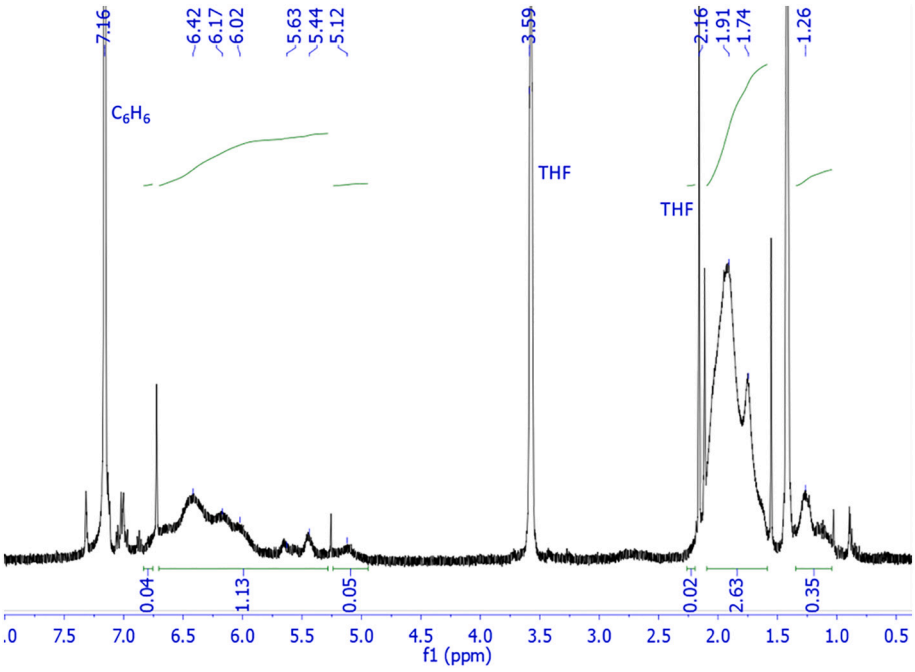

Fig. 2. ^{1}H NMR spectrum of soluble portion of *c*-A_{50}-P_{50} in C_6D_6 at 25 °C.

cyclic PA, *c*-A_{75}-P_{25}, *c*-A_{50}-P_{50}, and *c*-A_{25}-P_{75}.

2.9. SEM and EDS of the cyclic copolymers

Scanning electron microscope (SEM) images were obtained on a Tescan MIRA3 scanning electron microscope. The operating voltage ranged from 0.2 to 30 keV with a Schottky field emission gun ZrO/W source. Energy-dispersive X-ray spectroscopies (EDS) were collected using EDAX Octane Pro energy-dispersive spectroscopy (EDS) system. Fig. 5 depicts the SEM images of *c*-A_{75}-P_{25}, *c*-A_{50}-P_{50}, and *c*-A_{25}-P_{75}.

3. Results and discussion

Scheme 2 depicts the ring expansion polymerization (REP) for cyclic copolymers of acetylene and propyne with catalyst **1**. Previous studies confirmed the cyclic topology of the parent homopolymers, cyclic polyacetylene [19] and cyclic polypropyne [24]. In a similar approach to previous methods ([3,18]) coating a glass reactor with a thin layer of a solution of catalyst **1** (2 mg) in toluene and then exposing the reactor to various ratios of gaseous acetylene and propyne yields free-standing lustrous films of cyclic poly(acetylene-*co*-propyne). Films, ranging in

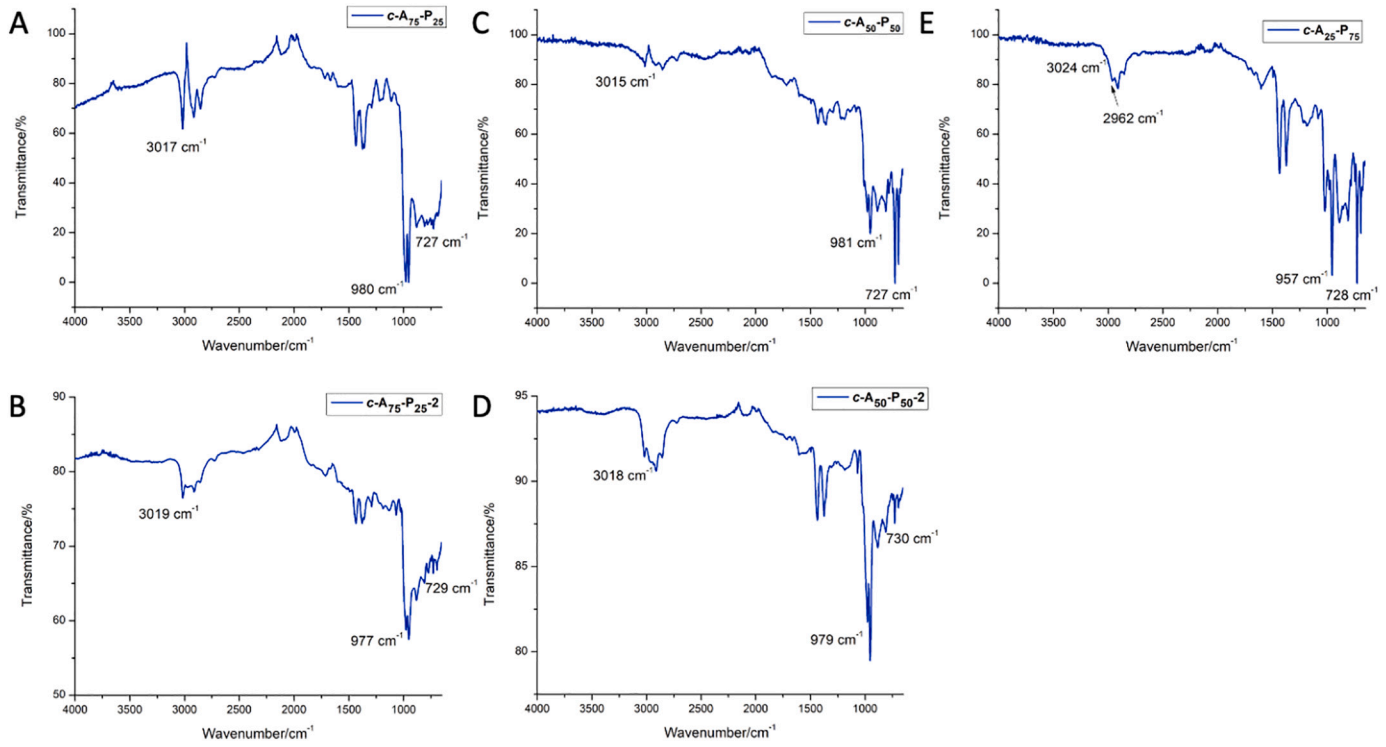

Fig. 3. IR spectra of (A) a *c*-A_{75}-P_{25} film (sample 1), (B) *c*-A_{75}-P_{25} film (sample 2), (C) a *c*-A_{50}-P_{50} film (sample 1), (D) *c*-A_{50}-P_{50} film (sample 2), (E) a *c*-A_{25}-P_{75} film.

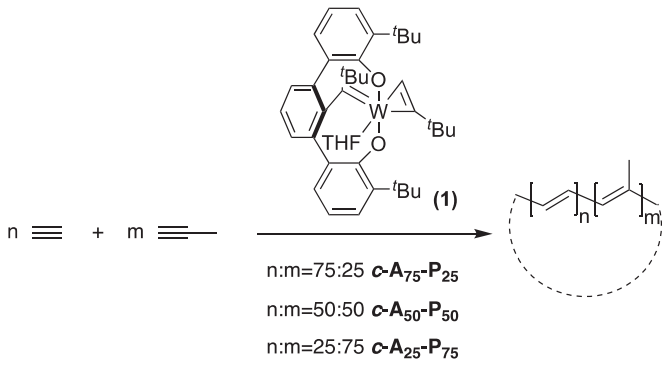

Scheme 2. Synthetic scheme of cyclic poly(acetylene-*co*-propyne).

color from black to deep-red, form immediately upon introducing the gas mixtures to the catalyst solution. Tailoring three gas compositions (acetylene: propyne = 75:25; 50:50; and 25:75) results in three films with varying acetylene/propyne content. With orders of magnitude lower catalyst loading (2 mg) compared to the cocatalyst system reported by Chien et al. (grams) [18], three simple washes of the resulting films with THF afford flexible, free-standing films of approximate composition *c*-A_{75}-P_{25}, *c*-A_{50}-P_{50}, and *c*-A_{25}-P_{75}. The naming convention of the cyclic copolymers indicates the ratios of acetylene and propyne in the starting gas mixtures, not necessarily the ratio of acetylene and propyne incorporation in the resulting cyclic copolymers. Without many other characterization techniques available, the metallic, lustrous appearance of polyacetylene films and their fibrillar morphology help confirm the successful synthesis [3,32,33] Shiny green/greenish-gold lustrous linear copolymers form using the Ti/Al method [18]. Fig. 4 depicts photographs of the copolymers that result using catalyst **1** after purification. Similar to polyacetylene, one surface of film *c*-A_{75}-P_{25} is lustrous and appears gold, while the other side is dull. SEM reveals the lustrous side of *c*-A_{75}-P_{25} film has a smooth macroscopic surface, while the dull side, unlike polyacetylene, displays no fibrillar textures. Instead, irregular "clumps" are observed that are similar to the linear copolymers synthesized by Chien et al. [18]. Less lustrous and black/green are films of *c*-A_{50}-P_{50} and *c*-A_{25}-P_{75}. For reference, pure homopolymers of cyclic polypropyne are orange [24]. We also observe that the decreased lustrous with the copolymers relates to their decreased conductivity that are discussed in later sections. Copolymer *c*-A_{50}-P_{50} does contain both a lustrous and dull side, whereas ac-A_{25}-P_{75} exhibits a dull black-silvery color on both sides. SEM of *c*-A_{50}-P_{50} also revealed a relatively smooth macroscopic surface on the shiny side and more irregular "clump" macrostructures on the dull side. Both *c*-A_{75}-P_{25} and *c*-A_{50}-P_{50} require no coating of conductive metals for SEM micrographs and display clear images as they are inherently semi-conductive, while SEM of *c*-A_{25}-P_{75} exhibits charging phenomenon due to its lower conductivity. SEM images of *c*-A_{25}-P_{75} also revealed a rough morphology.

A major advantage of using **1** to prepare copolymer films of acetylene and propyne is the ease of purification and low contaminations of residual metal impurities in the resulting polymers. Linear copolymers synthesized using the $Ti(O^nBu)_4/AlEt_3$ catalyst system require extensive washing to remove residual catalysts [18]. Energy Dispersive X-ray Spectroscopy (EDS) of the three cyclic copolymers revealed the films only contain 0.5–0.8 wt% residual W (Table 1) after three quick washes with THF. The observed oxygen contaminations in the copolymers are not surprising and are likely due to oxidation during the transfer of the samples to the EDS instrument, since acetylene/propyne copolymers exhibit higher air sensitivity compared to the cyclic homopolymers of both acetylene and propyne [18,34].

IR spectra of the copolymer films are useful for determining polyacetylene *cis/trans* configuration assignments [2]. Linear PA synthesized at −78 °C exhibits predominantly *cis* double bonds due to the consequence of the insertion mechanism of acetylene into a Ti-$C_{polymer}$ bond. Conducting the polymerization at >150 °C results in *cis* insertion and immediate isomerization to the thermodynamically stable *trans* configuration [2]. However, cyclic polyacetylene (*c*-PA) exhibits >99% *trans* double bonds regardless of the polymerization temperature, including as low as −94 °C. The low *cis-trans* isomerization barrier for *c*-PA is a consequence of rapid π-bond shifting and single bond rotation within a

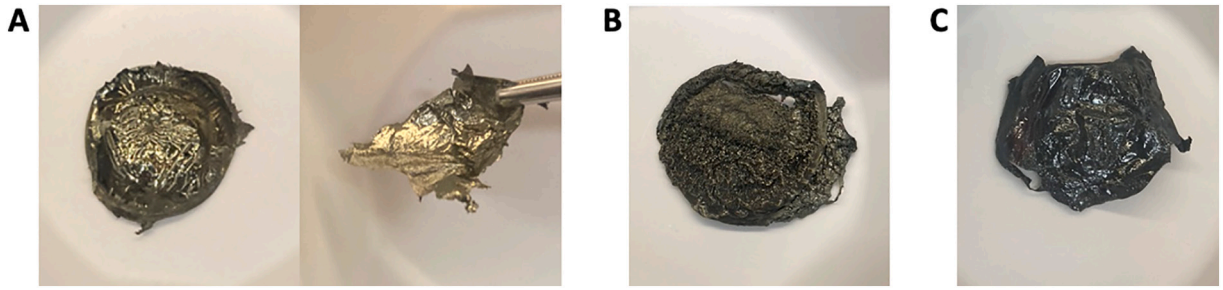

Fig. 4. Photographs of cyclic poly(acetylene-*co*-propyne) (**A**) *c*-A_{75}-P_{25} synthesized from 75:25 acetylene/propyne monomer feed; (**B**) *c*-A_{50}-P_{50} synthesized from 50:50 acetylene/propyne monomer feed; (**C**) *c*-A_{25}-P_{50} synthesized from 25:75 acetylene/propyne monomer feed.

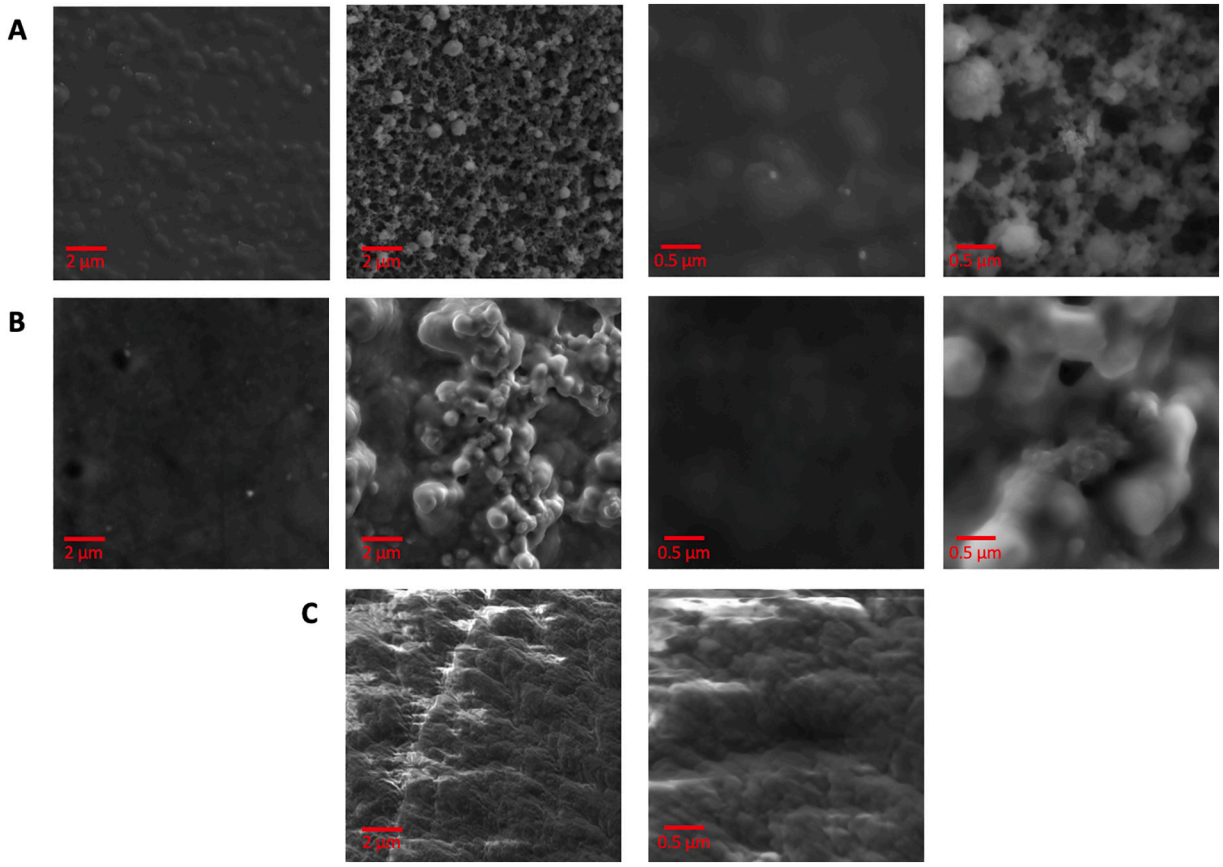

Fig. 5. SEM images of copolymers at two different scales. From left to right: (**A**) *c*-A_{75}-P_{25}, lustrous, 2 μm scale; *c*-A_{75}-P_{25} dull, 2 μm; *c*-A_{75}-P_{25} lustrous, 0.5 μm scale; *c*-A_{75}-P_{25} dull, 2 μm (**B**) *c*-A_{50}-P_{50}, lustrous. 2 μm; *c*-A_{50}-P_{50} dull, 2 μm; *c*-A_{50}-P_{50} lustrous. 0.5 μm; *c*-A_{50}-P_{50} dull, 0.5 μm; and (**C**) *c*-A_{25}-P_{75}, both sides are dull and exhibits similar morphology. Left is 2 μm scale and right is 0.5 μm scale.

Table 1
EDS-measured element relative percentages (H excluded) for cyclic copolymers.

Sample	C wt%	W wt%	O wt%
c-A_{75}-P_{25}-1	99.33	0.63	–
c-A_{50}-P_{50}-1	98.09	0.50	1.11
c-A_{25}-P_{75}-1	94.41	0.53	5.06
c-A_{75}-P_{25}*	97.49	0.64	1.86
c-A_{50}-P_{50}*	99.38	0.37	0.19
c-A_{25}-P_{75}*	96.19	0.60	3.21

* copolymer samples stored in sealed containers in a nitrogen filled glovebox over a few months.

highly conjugated ring; for example, [16]annulene exhibits this rapid configurational change above −50 °C [35]. Thus, *c*-PA, or [∞]annulene, will spontaneously isomerize to the *trans* isomer. One proposed requirement for the rapid isomerization is a highly conjugated cyclic backbone. As compared to *c*-PA, cyclic polyphenylacetylene contains mostly a *cis* configuration upon synthesis with catalyst **1** [20,23]. The bulky phenyl groups raise the barrier for efficient π-bond shifting within the ring, effectively trapping the *cis* configuration. IR spectra of the cyclic poly(acetylene-*co*-propyne) in this study reveal their mixed *cis* and *trans* configurations, depending on the propyne content (Fig. 6). The IR spectrum reveals an absorption at 980 cm^{-1} corresponding to the *trans* = C-H out-of-plane bending, whereas the *cis* = C-H out-of-plane bending absorbs at 728 cm^{-1}. Calculation of the % *cis* content based on Eq. (1) [3] for three distinct films suggests that *c*-A_{75}-P_{25} is 49% *cis*, and *c*-A_{50}-P_{50} and *c*-A_{25}-P_{50} are 66% and 69%, respectively. However,

these percentages determined by IR absorbance are not consistent, we observed a range of 5% to 70% *cis* content in various copolymer samples, where the *cis* percentage is not dependent on monomer feed ratio.

$$cis\% = 1.3A_{cis}/(1.3A_{cis} + A_{trans}) \quad (1)$$

Raman spectroscopy provides a second method for determining chain configuration [32,36,37]. Raman spectra of *c*-A_{75}-P_{25}, *c*-A_{50}-P_{50}, and *c*-A_{25}-P_{75} each exhibit clear bands near 1100 and 1500 cm^{-1} that are specific to *trans* PA [37], indicating a high degree of *trans* configuration for all three copolymer films (Fig. 7). The smaller, yet clear, absorptions at 1290 cm^{-1} are also attributable to a *trans* configuration. Unexpectedly, all three copolymers exhibit no obvious *cis* bands that are typically sharp and distinct at 920, 1250, and 1550 cm^{-1} [32,36]. For the higher-energy 532 nm laser, there is a shoulder on the 1500 cm^{-1} *trans* C=C stretch that can correspond to *cis* C=C configuration, but also to low conjugation length *trans* segments. However, without the sharp and intense absorption at 1250 cm^{-1}, it appears that there are few *cis* C=C bonds in the cyclic copolymers. There are additional absorptions at 860 cm^{-1} attributable to C=C-CH_3 stretching [38], but the frequencies for this mode are too close to distinguish between *cis* and *trans* isomers. Therefore, based on the Raman spectra, the copolymers adopt highly

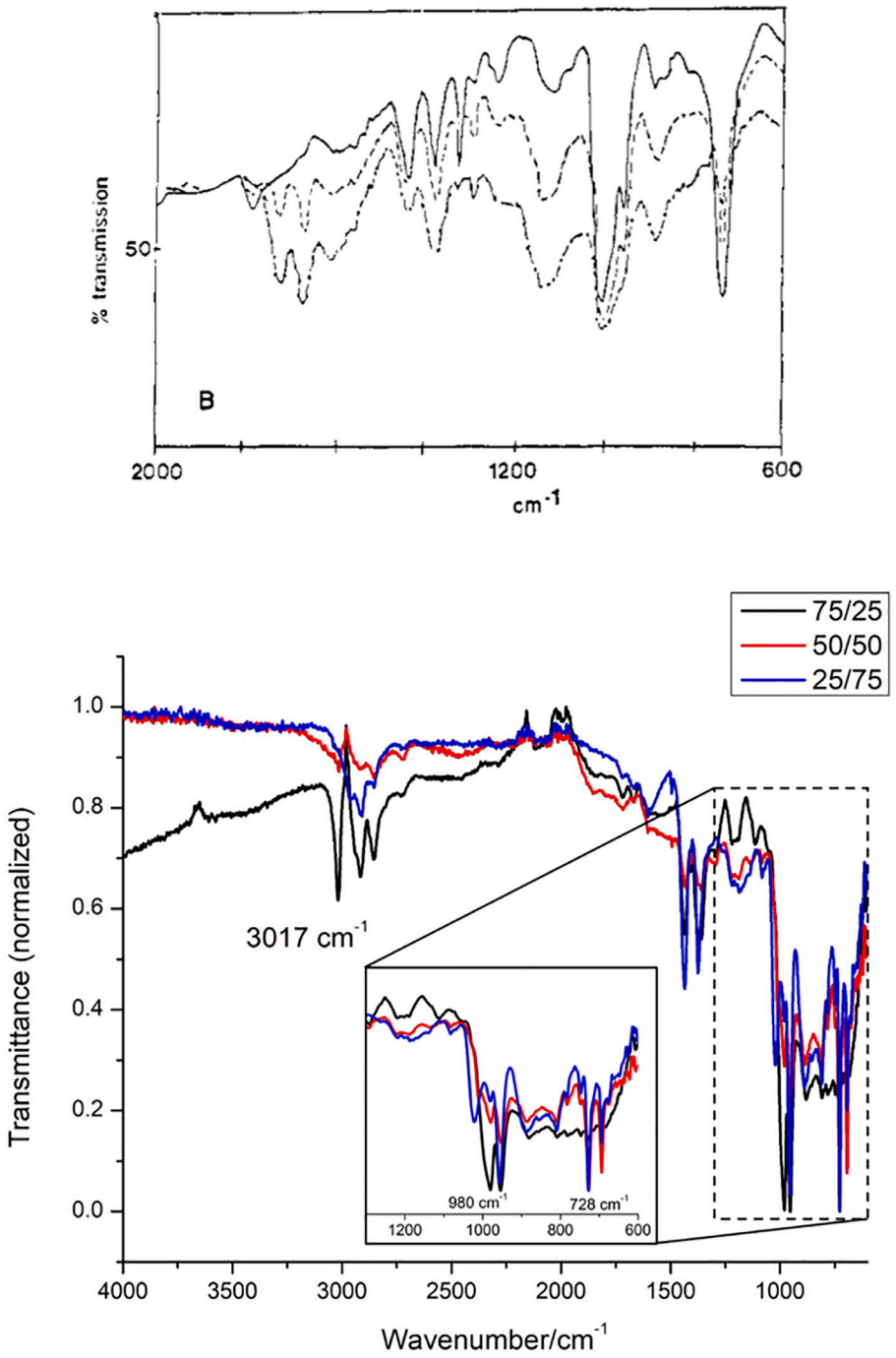

Fig. 6. Top: IR spectra of linear poly(acetylene-*co*-propyne) with 1:1 monomer feed ratio (solid line), reprinted with permission from ref. [11]. Copyright 1981 American Chemical Society. Bottom: *c*-A_{75}-P_{25} (black), *c*-$A_{50}P_{50}$ (red), and *c*-A_{25}-P_{75} (blue) copolymer films. (For interpretation of the references to colour in this figure legend, the reader is referred to the web version of this article.)

trans configurations. Yet, the reason for the disparity in *cis* and *trans* content of the same copolymers based on IR and Raman spectroscopy is unclear. A high-energy laser used for Raman spectroscopy might induce *cis-trans* isomerization at room temperature and lead to higher *trans* content in the films [32,36]. Alternatively, the *cis* segments could have low conjugation lengths beyond the excitation ranges for the lasers used in this study.

Copolymers with different acetylene/propyne content all exhibit conductivities below the detection limit of our 4-point probe station (10^{-6} Ω^{-1} cm^{-1}). Doping the films with I_2 for 3 h increases the conductivity by orders of magnitude. Doping for any longer, results in lower conductivities [19]. Unfortunately, the *c*-A_{25}-P_{75} copolymer becomes extremely brittle and breaks upon contact with the 4-point probe, making a conductivity measurement impossible. Table 2 summarizes the conductivity of two separate films of both *c*-A_{75}-P_{25} and *c*-A_{50}-P_{50} after doping.

Conductivity measurements fit closely to those of Chien et al. reported for linear acetylene/propyne copolymers [18]. The decrease in conductivity from *c*-A_{75}-P_{25} to *c*-A_{50}-P_{50} is consistent with lower conjugation lengths from increased propyne content. The methyl substituent, though small, must distort the local backbone planarity to avoid steric clash. This would decrease conjugation, and result in the observed decreased conductivity. At the same time, the copolymers with lower conductivities appear less lustrous.

Stirring the copolymers in THF overnight suspends the polymer as particles and dissolves 10 wt% of *c*-A_{75}-P_{25} and 28 wt% *c*-A_{50}-P_{50} in solution. ^{1}H NMR spectra of the soluble portions of the *c*-A_{75}-P_{25} and *c*-A_{50}-P_{50} films provides a quantitative measurement of propyne and acetylene monomer incorporation. These soluble fractions of *c*-A_{75}-P_{25} and *c*-A_{50}-P_{50} consist of only 9% and 10% acetylene (Figs. 1 and 2), respectively. The similar acetylene contents of the soluble portions from copolymers generated with different monomer feed suggest that solubility of the copolymers requires low acetylene incorporation, with a likely upper limit of ~10%.

Thermogravimetric analysis (TGA) of the copolymers and pure *c*-PA exhibit a trend in their decomposition temperatures (Fig. 8). TGA of *c*-PA reveals a 95% weight loss temperature of 360 °C, a close fit to reported values for the linear derivative [39]. Pure polypropyne is less thermally stable with a reported decomposition temperature between 180 and 200 °C [18]. Interestingly, the copolymers exhibit two decomposition processes, one in the range of 100–200 °C, close to that of pure polypropyne, and a second decomposition that approaches *c*-PA. With increased propyne content, the copolymers exhibit reduced thermal stabilities. Also signifying the change in propyne content, the weight loss percentage associated with the first process increases from *c*-A_{75}-P_{25} to *c*-A_{25}-P_{75}. Finally, the amount of residual char after TGA depends on the acetylene content [18]. Compared to *c*-A_{25}-P_{75} and *c*-$A_{50}P_{50}$, *c*-A_{75}-P_{25} has more residual material, whereas pure *c*-PA has the most at ~35 wt%, suggesting that copolymers with higher acetylene content indeed have more residue after pyrolysis.

Table 2
Conductivity of doped acetylene/propyne copolymers.

Sample	Thickness (μm)	Doping percentage of I_2 (wt%)	Conductivity (ohm^{-1} cm^{-1})
c-A_{75}-P_{25}-1	44.4	71.9	2.20
c-A_{75}-P_{25}-2	51.3	72.8	6.39
c-A_{50}-P_{50}-1	45.3	64.7	0.0110
c-A_{50}-P_{50}-2	48.7	65.5	0.0050

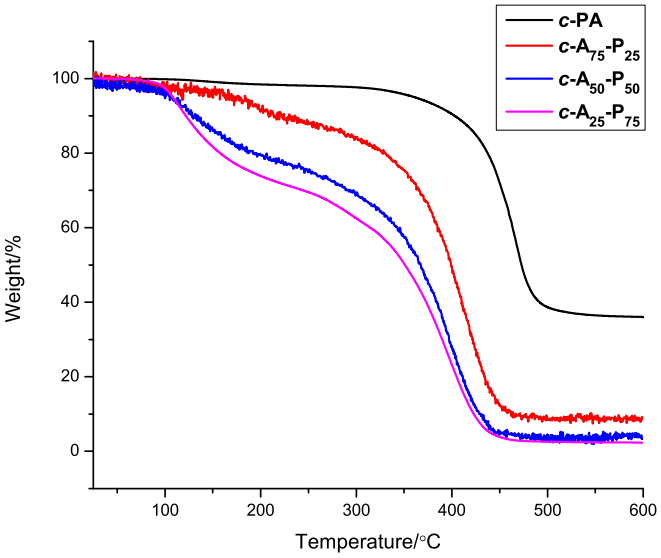

Fig. 8. TGA traces of cyclic polyacetylene (black), cyclic copolymer *c*-A_{75}-P_{25} (red), and cyclic copolymer *c*-A_{50}-P_{50} (blue), and cyclic copolymer *c*-A_{25}-P_{75} (purple). (For interpretation of the references to colour in this figure legend, the reader is referred to the web version of this article.)

4. Conclusion

This report describes a simple approach to the synthesis of cyclic poly (acetylene-*co*-propyne) as thin, flexible films. The low catalyst loading, and facile synthesis make the purification much easier compared to the linear copolymers. Controlling the monomer gas feed ratio alters the relative acetylene and propyne incorporation. With more acetylene content, the resulting copolymers exhibit more lustrous gold-like

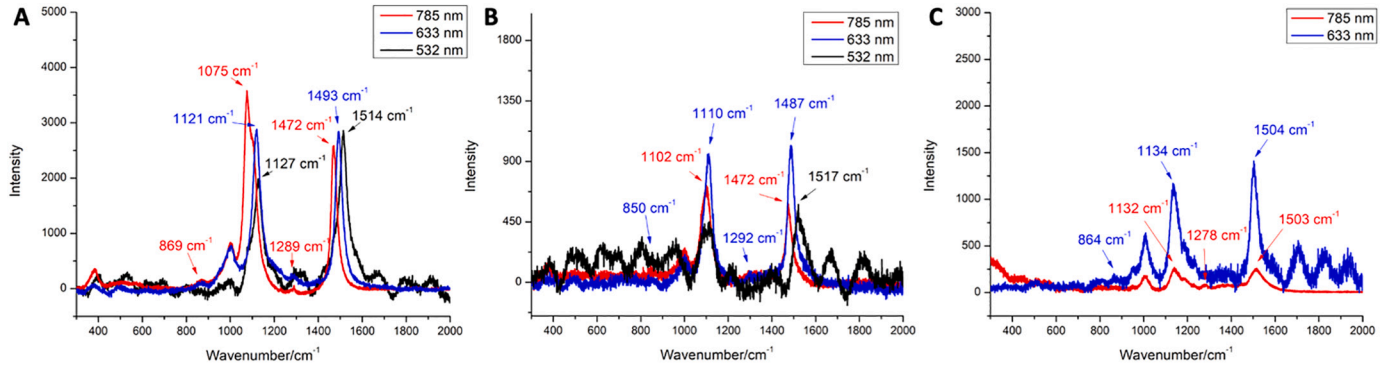

Fig. 7. Raman spectra of cyclic copolymer films (**A**) *c*-A_{75}-P_{25}, (**B**) *c*-A_{50}-P_{50}, and (**C**) *c*-A_{25}-P_{75} with 785, 633, and 532 nm excitation lasers (using 532 nm laser with *c*-A_{25}-P_{75} led to noise).

surfaces and higher thermal stabilities. Installation of a methyl group into polyacetylene increases the solubility and the ability to suspend the polymer in organic solvents, but it also decreases conjugation and, correspondingly, the conductivities. Preliminary conductivity data of iodine-doped cyclic copolymer films show moderate conductivity in the semi-conductor range. Overall, although the process for the synthesis of the cyclic copolymers is convenient, the copolymer solubility, thermal stability, and conductivity do not appear to be significantly influenced by the topology.

Declaration of Competing Interest

None.

Acknowledgments

This material is based upon work supported by the National Science Foundation CHE-1808234.

References

[1] G. Natta, G. Mazzanti, P. Corradini, Atti Accad. Naz. Lincei Rend. Cl. Sci. Fis. Mat. Nat. 25 (1958) 3.
[2] H. Shirakawa, S. Ikeda, Infrared spectra of poly(acetylene), Polym. J. 2 (1971) 231–244, https://doi.org/10.1295/polymj.2.231.
[3] T. Ito, H. Shirakawa, S. Ikeda, Simultaneous polymerization and formation of polyacetylene film on surface of concentrated soluble ziegler-type catalyst solution, J. Polym. Sci. A Polym. Chem. 12 (1974) 11–20, https://doi.org/10.1002/pola.1996.854.
[4] C.K. Chiang, M.A. Druy, S.C. Gau, A.J. Heeger, E.J. Louis, A.G. Macdiarmid, Y. W. Park, H. Shirakawa, Synthesis of highly conducting films of derivatives of polyacetylene, $(CH)_x$, J. Am. Chem. Soc. 100 (1978) 1013–1015, https://doi.org/10.1021/ja00471a081.
[5] N. Basescu, Z.X. Liu, D. Moses, A.J. Heeger, H. Naarmann, N. Theophilou, High electrical-conductivity in doped polyacetylene, Nature 327 (1987) 403–405, https://doi.org/10.1038/327403a0.
[6] J. Tsukamoto, A. Takahashi, Synthesis and electrical-properties of polyacetylene yielding conductivity of 10^5 s/cm, Synth. Met. 41 (1991) 7–12, https://doi.org/10.1016/0379-6779(91)90985-E.
[7] W.J. Feast, J. Tsibouklis, K.L. Pouwer, L. Groenendaal, E.W. Meijer, Synthesis, processing and material properties of conjugated polymers, Polymer 37 (1996) 5017–5047, https://doi.org/10.1016/0032-3861(96)00439-9.
[8] T.M. Swager, D.A. Dougherty, R.H. Grubbs, Strained rings as a source of unsaturation - polybenzvalene, a new soluble polyacetylene precursor, J. Am. Chem. Soc. 110 (1988) 2973–2974, https://doi.org/10.1021/ja00217a049.
[9] Z.X. Chen, J.A.M. Mercer, X.L. Zhu, J.A.H. Romaniuk, R. Pfattner, L. Cegelski, T. J. Martinez, N.Z. Burns, Y. Xia, Mechanochemical unzipping of insulating polyladderene to semiconducting polyacetylene, Science 357 (2017) 475–478, https://doi.org/10.1126/science.aan2797.
[10] J. Seo, S.Y. Lee, C.W. Bielawski, Unveiling a masked polymer of dewar benzene reveals trans-poly(acetylene), Macromolecules 52 (2019) 2923–2931, https://doi.org/10.1021/acs.macromol.8b02754.
[11] D.C. Bott, C.S. Brown, C.K. Chai, N.S. Walker, W.J. Feast, P.J.S. Foot, P.D. Calvert, N.C. Billingham, R.H. Friend, Durham polyacetylene - preparation and properties of the unoriented material, Synth. Met. 14 (1986) 245–269, https://doi.org/10.1016/0379-6779(86)90039-1.
[12] J.H. Edwards, W.J. Feast, D.C. Bott, New routes to conjugated polymers.1. A 2 step route to polyacetylene, Polymer 25 (1984) 395–398, https://doi.org/10.1016/0032-3861(84)90293-3.
[13] J.H. Edwards, W.J. Feast, A new synthesis of poly(acetylene), Polymer 21 (1980) 595–596, https://doi.org/10.1051/jphyscol:1983327.
[14] Z. Miao, D. Konar, B.S. Sumerlin, A.S. Veige, Soluble polymer precursors via remp for the synthesis of cyclic polyacetylene, Macromolecules 54 (2021) 7840–7848, https://doi.org/10.1021/acs.macromol.1c00938.
[15] T. Masuda, Substituted polyacetylenes: Synthesis, properties, and functions, Polym. Rev. 57 (2017) 1–14, https://doi.org/10.1080/15583724.2016.1170701.
[16] T. Masuda, T. Higashimura, Synthesis of high polymers from substituted acetylenes - exploitation of molybdenum-based and tungsten-based catalysts, Acc. Chem. Res. 17 (1984) 51–56, https://doi.org/10.1021/ar00098a002.
[17] C.B. Gorman, E.J. Ginsburg, R.H. Grubbs, Soluble, highly conjugated derivatives of polyacetylene from the ring-opening metathesis polymerization of monosubstituted cyclooctatetraenes - synthesis and the relationship between polymer structure and physical-properties, J. Am. Chem. Soc. 115 (1993) 1397–1409, https://doi.org/10.1021/ja00057a024.
[18] J.C. Chien, G.E. Wnek, F.E. Karasz, J.A. Hirsch, Electrically conducting acetylene-methylacetylene copolymers. Synthesis and properties, Macromolecules 14 (1981) 479–485, https://doi.org/10.1021/ma50004a004.
[19] Z. Miao, S.A. Gonsales, C. Ehm, F. Mentink-Vigier, C.R. Bowers, B.S. Sumerlin, A. S. Veige, Cyclic polyacetylene, Nat. Chem. 13 (2021) 792–799, https://doi.org/10.1038/s41557-021-00713-2.
[20] C. Roland, H. Li, K. Abboud, K. Wagener, A. Veige, Cyclic polymers from alkynes, Nat. Chem. 8 (2016) 791–796, https://doi.org/10.1038/nchem.2516.
[21] C.D. Roland, T. Zhang, S. VenkatRamani, I. Ghiviriga, A.S. Veige, A catalytically relevant intermediate in the synthesis of cyclic polymers from alkynes, Chem. Commun. 55 (2019) 13697–13700, https://doi.org/10.1039/C9CC05612B.
[22] S. Sarkar, K.P. McGowan, S. Kuppuswamy, I. Ghiviriga, K.A. Abboud, A.S. Veige, An OCO^{3-} trianionic pincer tungsten(vi) alkylidyne: Rational design of a highly active alkyne polymerization catalyst, J. Am. Chem. Soc. 134 (2012) 4509–4512, https://doi.org/10.1021/ja2117975.
[23] K.P. McGowan, M.E. O'Reilly, I. Ghiviriga, K.A. Abboud, A.S. Veige, Compelling mechanistic data and identification of the active species in tungsten-catalyzed alkyne polymerizations: conversion of a trianionic pincer into a new tetraanionic pincer-type ligand, Chem. Sci. 4 (2013) 1145–1155, https://doi.org/10.1039/C2SC21750C.
[24] W.J. Niu, S.A. Gonsales, T. Kubo, K.C. Bentz, D. Pal, D.A. Savin, B.S. Sumerlin, A. S. Veige, Polypropylene: now available without chain ends, Chem 5 (2019) 237–244, https://doi.org/10.1016/j.chempr.2018.12.005.
[25] Z.H. Miao, T. Kubo, D. Pal, B.S. Sumerlin, A.S. Veige, pH-responsive water-soluble cyclic polymer, Macromolecules 52 (2019) 6260–6265, https://doi.org/10.1021/acs.macromol.9b01307.
[26] D. Pal, Z.H. Miao, J.B. Garrison, A.S. Veige, B.S. Sumerlin, Ultra-high-molecular-weight macrocyclic bottlebrushes via post-polymerization modification of a cyclic polymer, Macromolecules 53 (2020) 9717–9724, https://doi.org/10.1021/acs.macromol.0c01797.
[27] Z.H. Miao, D. Pal, W.J. Niu, T. Kubo, B.S. Sumerlin, A.S. Veige, Cyclic poly(4-methyl-1-pentene): efficient catalytic synthesis of a transparent cyclic polymer, Macromolecules 53 (2020) 7774–7782. https://doi.org/10.1021/acs.macromol.0c01366.
[28] S.A. Gonsales, T. Kubo, M.K. Flint, K.A. Abboud, B.S. Sumerlin, A.S. Veige, Highly tactic cyclic polynorbornene: stereoselective ring expansion metathesis polymerization of norbornene catalyzed by a new tethered tungsten-alkylidene catalyst, J. Am. Chem. Soc. 138 (2016) 4996–4999, https://doi.org/10.1021/jacs.6b00014.
[29] S.S. Nadif, T. Kubo, S.A. Gonsales, S. VenkatRamani, I. Ghiviriga, B.S. Sumerlin, A. S. Veige, Introducing "ynene" metathesis: ring-expansion metathesis polymerization leads to highly cis and syndiotactic cyclic polymers of norbornene, J. Am. Chem. Soc. 138 (2016) 6408–6411, https://doi.org/10.1021/jacs.6b03247.
[30] V. Jakhar, D. Pal, I. Ghiviriga, K.A. Abboud, D.W. Lester, B.S. Sumerlin, A.S. Veige, Tethered tungsten-alkylidenes for the synthesis of cyclic polynorbornene via ring expansion metathesis: unprecedented stereoselectivity and trapping of key catalytic intermediates, J. Am. Chem. Soc. 143 (2021) 1235–1246, https://doi.org/10.1021/jacs.0c12248.
[31] K. Nakao, M. Nishimura, T. Tamachi, Y. Kuwatani, H. Miyasaka, T. Nishinaga, M. Iyoda, Giant macrocycles composed of thiophene, acetylene, and ethylene building blocks, J. Am. Chem. Soc. 128 (2006) 16740–16747, https://doi.org/10.1021/ja067077t.
[32] H. Shirakawa, T. Ito, S. Ikeda, Raman-scattering and electronic-spectra of poly (acetylene), Polym. J. 4 (1973) 460–462, https://doi.org/10.1295/polymj.4.460.
[33] H. Shirakawa, E.J. Louis, A.G. Macdiarmid, C.K. Chiang, A.J. Heeger, Synthesis of electrically conducting organic polymers - halogen derivatives of polyacetylene, $(CH)_x$, J. Chem. Soc.-Chem. Comm. (1977) 578–580, https://doi.org/10.1039/C39770000578.
[34] J.C.W. Chien, L.C. Dickinson, X. Yang, Autoxidation and stabilization of poly (methylacetylene), Macromolecules 16 (1983) 1287–1295, https://doi.org/10.1021/ma00242a007.
[35] C.S. Michel, P.P. Lampkin, J.Z. Shezaf, J.F. Moll, C. Castro, W.L. Karney, Tunneling by 16 carbons: planar bond shifting in [16]annulene, J. Am. Chem. Soc. 141 (2019) 5286–5293, https://doi.org/10.1021/jacs.8b13131.
[36] L.S. Lichtmann, D.B. Fitchen, H. Temkin, Resonant raman-spectroscopy of conducting organic polymers - (ch)x, and an oriented analog, Synth. Met. 1 (1980) 139–149, https://doi.org/10.1016/0379-6779(80)90005-3.
[37] I. Harada, M. Tasumi, H. Shirakawa, S. Ikeda, Raman-spectra of polyacetylene and highly conducting iodine-doped polyacetylene, Chem. Lett. (1978) 1411–1414, https://doi.org/10.1246/cl.1978.1411.
[38] Y. Koyama, Y. Mukai, J. Umemura, M. Ito, K. Tsukida, Raman and infrared-spectra of the 7-cis and di-cis isomers of retinal, J. Raman Spectrosc. 15 (1984) 300–307, https://doi.org/10.1002/jrs.1250150503.
[39] J.C.W. Chien, P.C. Uden, J.L. Fan, Pyrolysis of polyacetylene, J. Polym. Sci. A Polym. Chem. 20 (1982) 2159–2167, https://doi.org/10.1002/pol.1982.170200819.